

Polarization of “water-skies” above arctic open waters: how polynyas in the ice-cover can be visually detected from a distance

Ramón Hegedüs

*Biooptics Laboratory, Department of Biological Physics, Physical Institute, Loránd Eötvös University,
H-1117 Budapest, Pázmány Péter sétány 1, Hungary*

Susanne Åkesson

Department of Animal Ecology, Lund University, Ecology Building, SE-223 62 Lund, Sweden

Gábor Horváth

*Biooptics Laboratory, Department of Biological Physics, Physical Institute, Loránd Eötvös University,
H-1117 Budapest, Pázmány Péter sétány 1, Hungary*

Received March 17, 2006; revised June 29, 2006; accepted July 19, 2006;
posted August 17, 2006 (Doc. ID 69079); published December 13, 2006

The foggy sky above a white ice-cover and a dark water surface (permanent polynya or temporary lead) is white and dark gray, phenomena called the “ice-sky” and the “water-sky,” respectively. Captains of icebreaker ships used to search for not-directly-visible open waters remotely on the basis of the water sky. Animals depending on open waters in the Arctic region may also detect not-directly-visible waters from a distance by means of the water sky. Since the polarization of ice-skies and water-skies has not, to our knowledge, been studied before, we measured the polarization patterns of water-skies above polynyas in the arctic ice-cover during the Beringia 2005 Swedish polar research expedition to the North Pole region. We show that there are statistically significant differences in the angle of polarization between the water-sky and the ice-sky. This polarization phenomenon could help biological and man-made sensors to detect open waters not directly visible from a distance. However, the threshold of polarization-based detection would be rather low, because the degree of linear polarization of light radiated by water-skies and ice-skies is not higher than 10%. © 2006 Optical Society of America

OCIS codes: 010.1290, 110.2960, 120.5410, 280.1310, 330.7310.

1. INTRODUCTION

In the ice-cover of the Arctic Ocean there are long or short, wide or narrow, permanent or temporary open water surfaces, especially in the summer. These open waters are called polynyas (when permanent, long, and wide) or leads (when temporary, short, and narrow) and are of great importance to animal life in the arctic^{1–3} and antarctic⁴ regions. According to Tomas Arnell, captain of the Swedish icebreaker Oden, captains of icebreaker ships prefer to follow the line of such polynyas and leads, because then the ship can move faster and more easily. The open water surfaces can be visually detected on the basis of their low albedo (reflectivity): Polynyas and leads occur as dark gray or black stripes in the high-albedo (white) ice field (Fig. 1A). Above the upstreaming warmer water of polynyas, rising vapor occurs frequently (Fig. 1B). If the sky is foggy, the sky above dark water surfaces is always dark gray (Figs. 1C–1E). This phenomenon is called the “water-sky.” On the other hand, the foggy sky above high-albedo ice/snow surfaces is always white (Figs. 1A–1E), which is called the “ice-sky.” Hence, at the ice–

water border of polynyas and leads there is a difference in radiance between the ice-sky and the water-sky (Figs. 1C and 1D). Thus, polynyas and leads can be remotely detected by means of this celestial radiance difference by means of the dark gray band (Figs. 1E and 1F) of the water-sky, even if the water surface is not visible because of the curvature of the Earth’s surface. Figure 2 shows schematically the geometry of a remote (Fig. 2A) and a near (Fig. 2B) view of a water-sky above a polynya seen from an icebreaker. The captains of icebreakers in the Arctic Ocean used to search for open waters in such a way.⁵ According to Sven Stenvall, helicopter pilot, the pilots of helicopters of icebreakers also use this information during ice reconnaissance flights above the arctic ice-cover.

Polar bears and several seabird species in the arctic region are strongly dependent on the existence of open waters (leads and polynyas), because their prey (mainly seals for polar bears, fish and invertebrates for birds) originate from the seawater.^{3,6–10} Animals inhabiting the arctic ice landscape could possibly, like captains of ice–

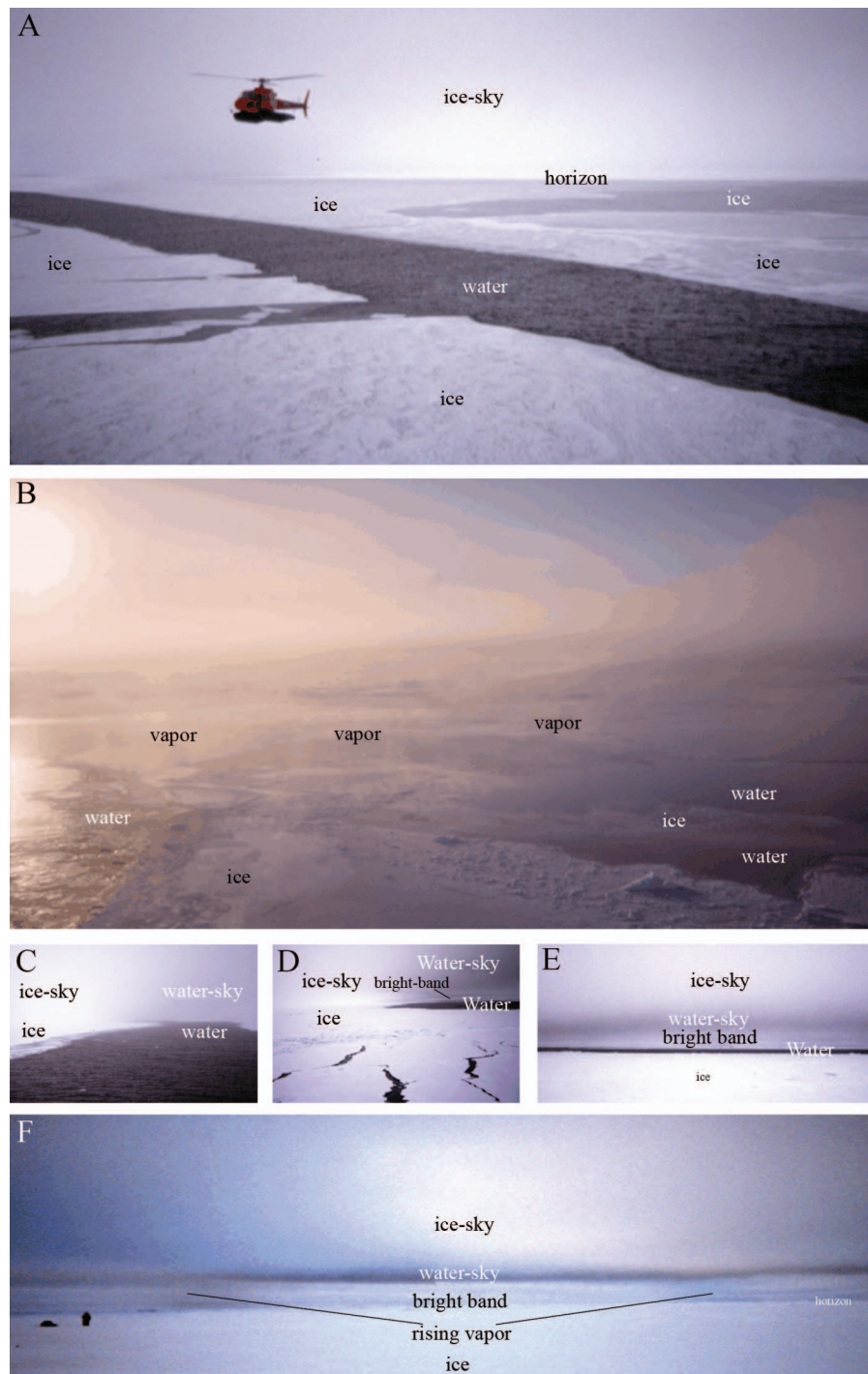


Fig. 1. A, Typical low-albedo (dark) open water surface (polynya) in the high-albedo (white) arctic ice-cover. The helicopter was stationed on board the Swedish icebreaker Oden and was used for ice reconnaissance flights. B, Rising vapor above the upstreaming warmer water of a polynya. C, D, Typical white “ice-skies” and gray “water-skies” above the arctic ice broken with polynyas. E, Above a long straight distant polynya visible near the horizon a long water-sky occurs. F, An elongated horizontal water-sky above a long straight polynya that is not visible because of the curvature of the Earth’s surface. The two darker spots between the water-sky and the horizon are water vapor clouds rising from two warmer spots of the polynya’s water surface. Not-directly-visible remote open waters can be detected from a distance on the basis of the smaller radiance of light from water-skies visible above them.

breakers, detect open waters from a distance on the basis of the dark gray water-sky. As far as we know, this hypothesis has not been tested behaviorally up to now. On the other hand, certain arctic birds may also be sensitive to polarized light, like several other bird species using sky polarization for orientation.¹¹

As far as we know, up to now the polarization of light from ice-skies and water-skies has not been studied. To fill this gap, we measured the polarization patterns of water-skies above polynyas in the arctic ice-cover during the Beringia 2005 Swedish polar research expedition to the Arctic Ocean. We present here some typical celestial

polarization patterns occurring above the arctic ice broken by polynyas. We show that there are statistically significant differences in the angle of polarization between the water-sky and the ice-sky radiating light with low degrees of linear polarization.

2. MATERIALS AND METHODS

We participated in the third part (Leg 3) of the international arctic research expedition “Beringia 2005” organized by the Swedish Polar Research Secretariat between 15 August and 25 September 2005. During this expedition

the Arctic Ocean was crossed by the Swedish icebreaker Oden approximately along a longitudinal great circle from Barrow (Alaska, $71^{\circ} 19' \text{ N}$) to Longyearbyen (Svalbard, Spitsbergen, 78° N). The icebreaker frequently followed the line of polynyas and leads, and it stopped periodically to perform different oceanographic samplings and measurements. Our polarimetric measurements and photography (Figs. 1, 3, and 4) were done on 11 September 2005 from the uppermost deck (at a height of about 15 m from the sea surface) of the icebreaker Oden when the ship stopped at the border of two polynyas (first polynya: $89^{\circ} 14.6' \text{ N}$, $174^{\circ} 2' \text{ W}$, 01:50 local summer time=UTC-8;

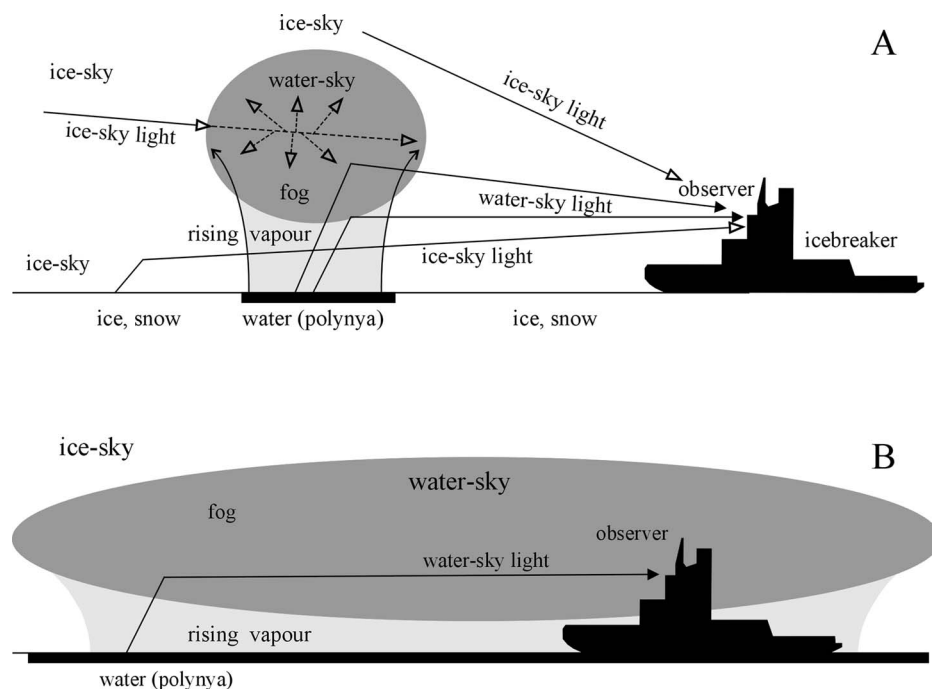


Fig. 2. Remote (A) and near (B) views of a water-sky above a polynya seen from an icebreaker. Light from the water-sky and the ice-sky is represented by black- and white-headed arrows, respectively. The strong scattering and absorption of ice-sky light in the fog cloud above the water surface is symbolized by dashed lines.

Table 1. Number of Pixels and Optical Characteristics (Average \pm Standard Deviation) of Light from Different Sections of the Arctic Sky Shown in Fig. 3^a

Image Section	Number of Pixels	Relative Radiance $i(\%)$			Degree of Linear Polarization $d(\%)$			Angle of Polarization $\alpha(^{\circ})$		
		Red	Green	Blue	Red	Green	Blue	Red	Green	Blue
Whole sky	117,500	58 ± 5	52 ± 4	80 ± 6	5 ± 3	5 ± 3	4 ± 2	41 ± 24 ($t=47.4$)	41 ± 24 ($t=43.1$)	34 ± 23 ($t=63.0$)
Ice	23,500	52 ± 4	48 ± 3	72 ± 5	5 ± 3	5 ± 3	4 ± 3	53 ± 23 ($t=22.1$)	52 ± 22 ($t=20.8$)	49 ± 24 ($t=27.6$)
Water-sky	2700	56 ± 2	49 ± 2	74 ± 4	4 ± 2	5 ± 2	4 ± 2	63 ± 15 ($t=74.1$)	61 ± 14 ($t=140.7$)	62 ± 14 ($t=203.1$)
Ice-sky	45,900	61 ± 3	55 ± 2	84 ± 2	6 ± 2	5 ± 3	4 ± 2	22 ± 14 ($t=87.5$)	22 ± 14 ($t=60.2$)	17 ± 11 ($t=62.5$)
Bright band	1530	62 ± 2	55 ± 2	83 ± 3	4 ± 3	5 ± 4	4 ± 3			

^aThe angle of polarization $\alpha(^{\circ})$ is measured from the vertical. The relative radiance is $i=I/I_{\max}$, where I is the measured radiance and I_{\max} is the maximum radiance in the picture. “Whole sky” and “ice” mean the entire upper half and lower part of the picture, respectively. The regions of “water-sky,” “ice-sky” and “bright band” are shown in Fig. 3(A) by rectangles. All α values are statistically significantly different (t test for two independent samples: $p < 0.001$) from those of the water-sky (bold). The statistical t values are given in parentheses.

Table 2. As Table 1 but for Fig. 4^a

Image Section	Number of Pixels	Relative Radiance $i(\%)$			Degree of Linear Polarization $d(\%)$			Angle of Polarization $\alpha(^{\circ})$		
		Red	Green	Blue	Red	Green	Blue	Red	Green	Blue
Whole sky	119,200	62±8	51±6	67±8	5±3	5±3	5±3	43±23 ($t=69.6$)	43±23 ($t=53.4$)	39±23 ($t=72.1$)
Ice	21,900	65±5	53±4	68±4	4±3	4±3	4±3	64±20 ($t=14.7$)	59±22 ($t=10.6$)	58±23 ($t=20.4$)
Water-sky	3850	47±5	38±3	49±4	6±4	6±4	5±3	69±16	63±19	66±19
Ice-sky	74,700	66±6	54±4	71±5	6±4	5±3	5±3	38±21 ($t=90.3$)	38±21 ($t=72.4$)	34±20 ($t=97.1$)
Bright band	70	49±3	38±3	51±3	4±2	5±3	4±2	54±19 ($t=7.8$)	43±24 ($t=8.7$)	48±20 ($t=7.9$)

^aAll α values are again statistically significantly different (t test for two independent samples: $p < 0.001$) from those of the water-sky (bold). The statistical t values are given in parentheses.

second polynya: 89° 15.5' N, 172° 22.6' W 07:30), and the sky was foggy; thus a striking white ice-sky and a dark gray water-sky occurred above the water surface.

The sky light polarization was measured by 180° field-of-view imaging polarimetry, which is described in detail by Gál *et al.*¹² Here we mention only that a 180° field of view was ensured by a fisheye lens (Nikon–Nikkor, $F = 2.8$, focal length 8 mm) with a built-in rotating filter wheel mounted with three broadband (275–750 nm) neutral density linearly polarizing filters (Polaroid HNP'B) with three different polarization axes (0°, 45°, and 90° from the radius of the wheel). The detector was a photo emulsion (Kodak Elite Chrome ED 200 ASA color reversal film; the maxima and half-bandwidths of its spectral sensitivity curves were $\lambda_{\text{red}} = 650 \pm 40$ nm, $\lambda_{\text{green}} = 550 \pm 40$ nm, $\lambda_{\text{blue}} = 450 \pm 40$ nm) in a roll-film photographic camera (Nikon F801). For a given scene, three photographs were taken for the three different directions of the transmission axis of the polarizers. The camera was set on a tripod such that the optical axis of the fisheye lens was horizontal. Using a personal computer, after evaluation of the three chemically developed color pictures for a given sky and 24-bit (3×8 for red, green and blue) digitization (using a Canon Arcus 1200 scanner), the patterns of the radiance I , degree of linear polarization d , and angle of polarization α of light were determined as color-coded, two-dimensional, circular maps. These patterns were obtained in the red, green, and blue spectral ranges, in which the three color-sensitive layers of the photo emulsion used have maximum sensitivity. The degree d and angle α of linear polarization were measured by our polarimeter with an accuracy of $\Delta d = \pm 1\%$ and $\Delta \alpha = \pm 2^{\circ}$, respectively. The average α values of different sky sections (Tables 1 and 2) were compared by paired t test with the use of the computer program STATISTICA 6.1.

3. RESULTS

As an example, results from polarimetric measurements are shown in Fig. 3, including a color photograph of the view being analyzed and the patterns of the degree of linear polarization d and the angle of polarization α of the sky above the arctic ice with a polynya stretching nearly parallel to the horizon measured by 180° field-of-view im-

aging polarimetry in the blue (450 nm) part of the spectrum. Since the polarization patterns measured in the red (650 nm) and the green (550 nm) parts of the spectrum were very similar to those in the blue, we do not present them here. Due to the very high (approximately 90%) albedo of snowy ice, the white ice surface is nearly as bright as the white ice-sky above the ice-cover (Fig. 3A, Table 1). Above the low-albedo (dark) water surface of the polynya the foggy sky is gray, which is called the “water-sky.” The brightness (radiance) of the water-sky is smallest at its lower part and gradually increases upward up to that of the ice-sky. Thus, on top of the fisheye picture (towards the zenith) there is no sharp border between the ice-sky and the water-sky. On the other hand, the water-sky does not begin immediately above the water surface: There is a bright horizontal celestial band between the water and the water-sky. The border between this celestial “bright band” and the lowermost part of the water-sky is sharp (Fig. 3A), and there is a moderate radiance difference between the bright band and the water-sky: Depending on the wavelength, the differences in the relative radiances i between them are $i_{\text{bright band}} - i_{\text{water-sky}} = 6\% - 9\%$ (Table 1).

According to Fig. 3B and Table 1, the average degree of linear polarization d of light from the ice-sky (4%–6%) is as low as that of the ice-reflected light (4%–5%) and the light from the water-sky (4%–5%), while the water surface of the polynya reflects light with the highest polarization, d (20%–25%). Thus, the water-sky cannot be discerned from the ice-sky in the d pattern in Fig. 3B.

In Fig. 3C and Table 1, we can see that there are statistically significant differences (paired t -test: $p < 0.001$) in the angle of polarization α between the water-sky and the ice-sky above and the celestial bright band below: Depending on the wavelength, the α values of light from the water-sky are $61^{\circ} - 63^{\circ} \pm 14^{\circ} - 15^{\circ}$ (shaded by green and blue colors in Fig. 3C), while the α values of light from the ice-sky above the water-sky and from the celestial bright band below the water-sky are $17^{\circ} - 22^{\circ} \pm 11^{\circ} - 14^{\circ}$ and $30^{\circ} - 34^{\circ} \pm 18^{\circ} - 20^{\circ}$, respectively (shaded by red and yellow colors in Fig. 3C). Analyzing the α patterns measured in the red, green, and blue parts of the spectrum (in Fig. 3C the α pattern is shown only in the blue), we can establish that the area of the celestial region with nearly vertical direc-

tions of polarization (with angle of polarization $-45^\circ < \alpha < +45^\circ$ shaded by red and yellow in Fig. 3C) is the larger the shorter the wavelength; furthermore, the sky light and the light reflected from the smooth horizontal ice surface are nearly horizontally polarized (with angle of polarization $+45^\circ < \alpha < +135^\circ$ shaded by green and blue in Fig. 3C) at the left and right side of the 180° field-of-view scene.

As another example, the optical characteristics of another scene with a water-sky are shown in Fig. 4. Here the left half of the 180° field-of-view of the camera is filled by the ice-cover and the ice-sky above it, while the right

half is filled by the dark water surface of a polynya and by the gray water-sky, which gradually transforms upward into the bright ice-sky. In this case again there is a celestial bright band below the gray water-sky (Fig. 4A), the average d of light from the water-sky (5%–6%) is as low as that of its surroundings (Fig. 4B, Table 2), and the celestial region with nearly vertical directions of polarization increases with decreasing wavelength (in Fig. 4C again the α pattern is shown only in the blue). According to Fig. 4C and Table 2, the differences in α between the celestial bright band ($\alpha=43^\circ-54^\circ \pm 19^\circ-24^\circ$), the water-sky ($\alpha=63^\circ-69^\circ \pm 16^\circ-19^\circ$), and the ice-sky (α

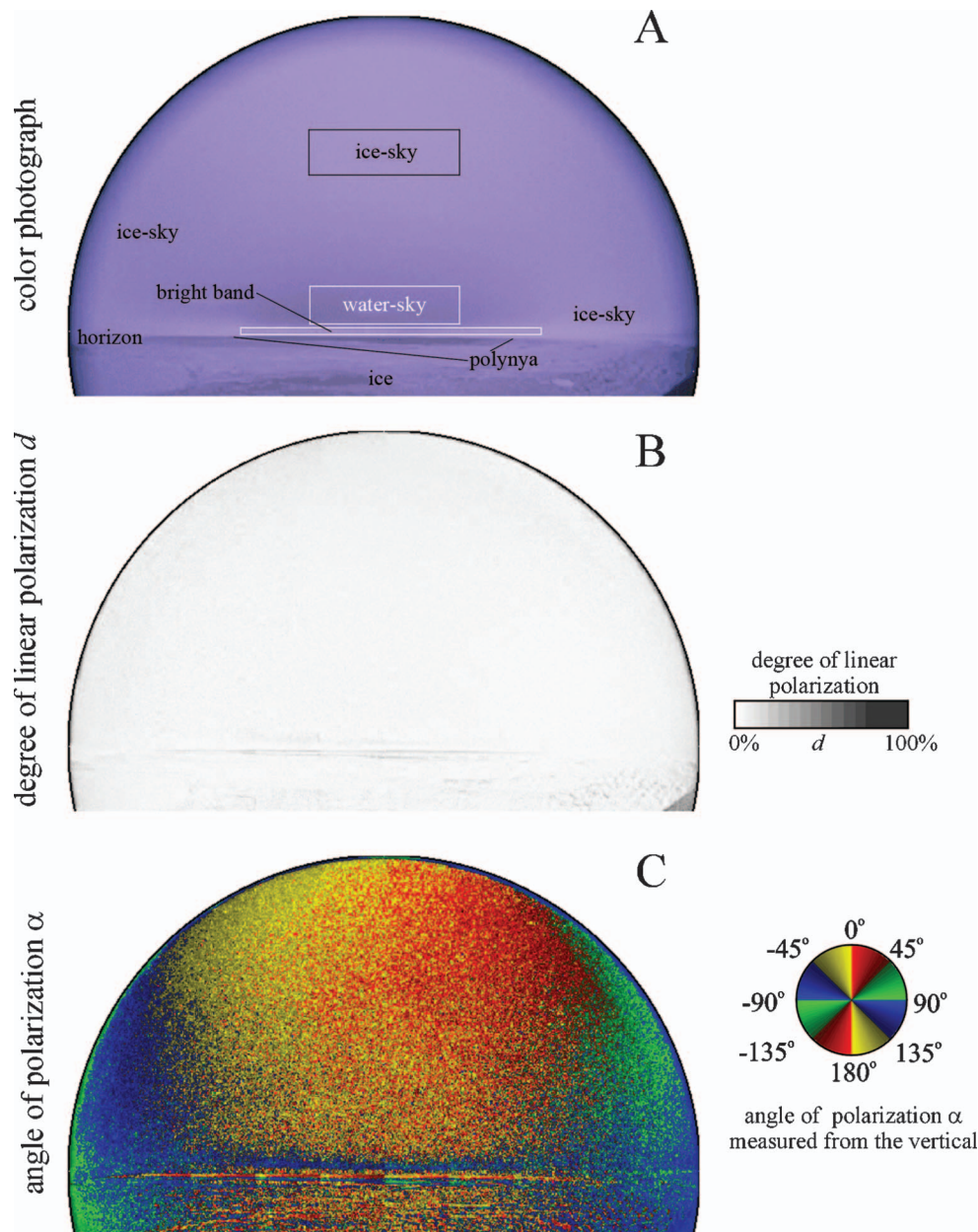


Fig. 3. A, 180° field-of-view color photograph of the sky above the arctic ice with a polynya stretching nearly parallel to the horizon in the middle part of the picture on 11 September 2005 at 01:50 (local summer time=UTC–8) at the geographical coordinates $89^\circ 14.6' \text{ N}$ and $174^\circ 2' \text{ W}$. B, C, Patterns of the degree of linear polarization d and the angle of polarization α of the sky measured by 180° field-of-view imaging polarimetry in the blue (450 nm) part of the spectrum. These patterns are very similar to those measured in the green (550 nm) and red (650 nm) parts of the spectrum. The optical axis of the fisheye lens was horizontal; thus the horizon is the horizontal diameter of the circular picture, the upper and lower parts of which show the sky and the ice-cover with a polynya, respectively. Only a fraction of the ice surface is shown. The rectangles in A show the celestial regions for which the values in Table 1 were calculated.

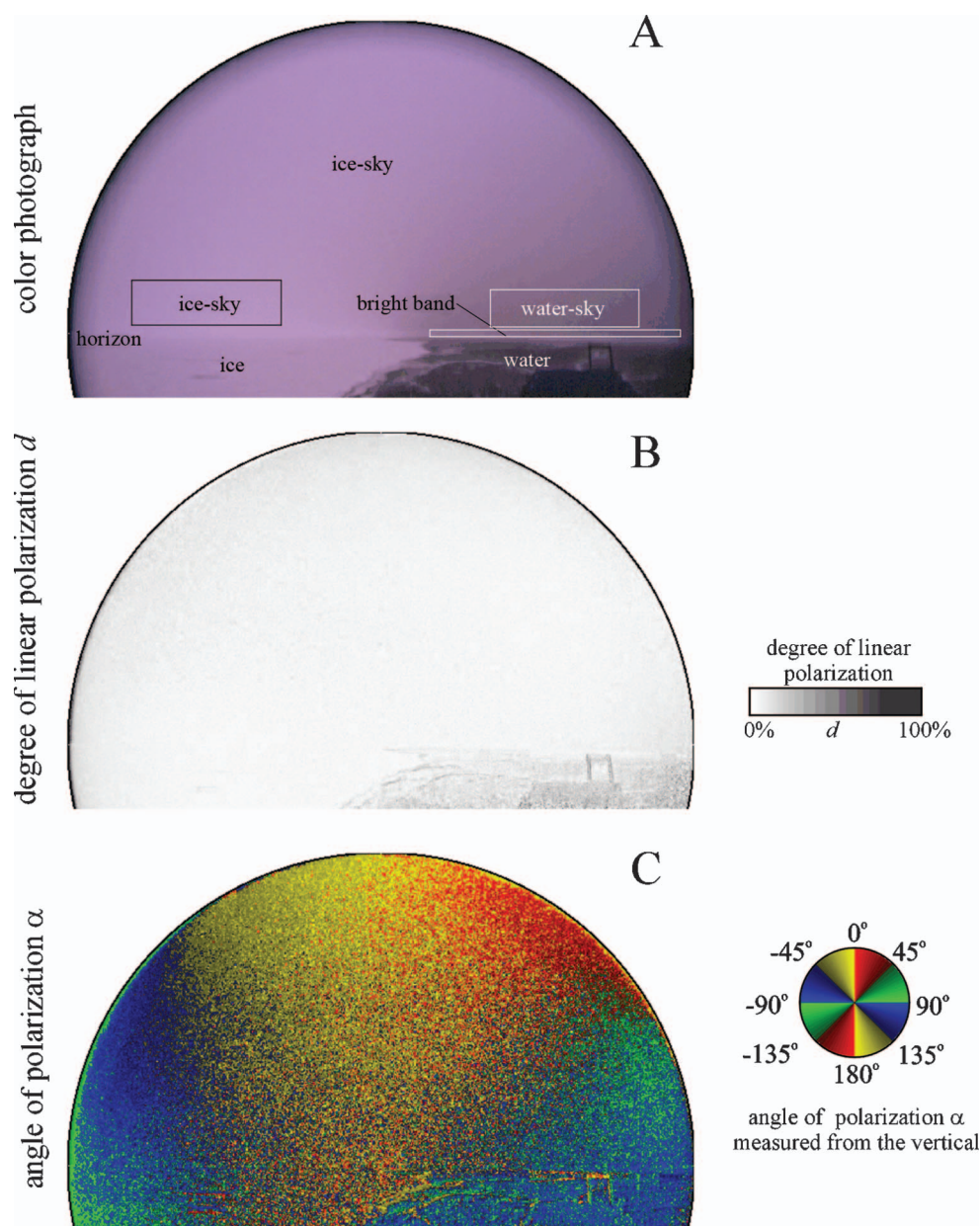


Fig. 4. As Fig. 3, but in this example ($89^{\circ} 15.5' \text{ N}$, $172^{\circ} 22.6' \text{ W}$, $07:30 = \text{UTC} - 8$) the statistically significant differences in the angle of polarization α between the ice-sky and the water-sky are smaller. The rectangles in A show the celestial regions for which the values in Table 2 were calculated.

$= 34^{\circ} - 38^{\circ} \pm 20^{\circ} - 21^{\circ}$) are again statistically significant (paired t test: $p < 0.001$), but they are smaller than those in Fig. 3. Figure 2A illustrates how the water-skies visible in Figs. 3 and 4 were generated and seen from the ice-breaker Oden. Quite similar results were obtained for four other arctic skies (with water-sky) above polynyas.

4. DISCUSSION

Polynyas rise where the warm seawater of constant currents of the Arctic Ocean streams up. From the water surface of polynyas water vapor rises (Fig. 1B), and after the condensation of the vapor a cloud of water fog arises. In Fig. 1F two darker spots of the rising and partially condensed water vapor are visible. The light from the bright ice-sky can reach a remote observer either above or below

the fog cloud above a polynya. The horizontal celestial bright band below the gray water-sky is due to the bright ice-sky light reaching the observer through the more-or-less transparent rising vapor below the fog cloud (Figs. 2A, 3, and 4). Thus, the light from this bright band has approximately the same radiance and polarization as the original ice-sky light. The radiance I of light from the bright band is as high as that from the surrounding ice-sky (Figs. 3A and 4A). In Figs. 3B and 4B the degree of linear polarization d of the bright band is as low as that of the ice-sky, while in Figs. 3C the light from the bright band is nearly vertically polarized ($-45^{\circ} < \alpha < +45^{\circ}$ shaded by red and yellow), like the background ice-sky light. Similarly, in Figs. 4C the light from the bright band is nearly horizontally polarized ($+45^{\circ} < \alpha < +135^{\circ}$ shaded by green and blue) as is the background ice-sky light.

When the lowest part of the water-sky is seen below the horizon, there is no celestial bright band below the water-sky. This is the situation in Figs. 1B and 1C, where the icebreaker was positioned in the fog cloud above a polynya (Fig. 2B). In Fig. 1A there is no water surface next to the horizon; thus neither water-sky nor bright band is visible. The bright band can be clearly seen in Figs. 1D–1F, 3 and 4, where the situation was the same as shown in Fig. 2A.

From Figs. 1 and 2 it is apparent that perception of both radiance and polarization differences between water-skies and ice-skies depends on the observer's height above ground. Thus it depends also on whether the observer is on the ice or in the water: A polar bear rearing up on its hind legs might stand 3 m tall, the observer on the icebreaker Oden was 15 m high up, and an arctic bird might be flying 150 m or more above the Arctic Ocean. However, since the mentioned radiance and polarization differences could be important only from remote distances (several tens of kilometers) in the detection of not-directly-visible water surfaces, the relatively small (from a few to 100 meters) height of the observer is irrelevant.

The fog cloud above a polynya considerably attenuates (absorbs and scatters) the light from the background ice-sky. On the other hand, due to the very low albedo (5%–10%) of the arctic water surface, only a small amount of light is reflected upward from the polynya toward the fog cloud; consequently, only a small amount of polynya-reflected light can be scattered by the fog toward the observer. These are the reasons for the small radiance of light coming from the gray water-sky, i.e., from the fog cloud above a polynya. This small radiance of water-skies is demonstrated in Figs. 1, 3A, and 4A. The polarization characteristics of water-skies are determined predominantly by the polarization of light reflected from the water surface such that the polynya-reflected light is always horizontally polarized with a degree of linear polarization depending on the angle of reflection. This horizontally polarized polynya-reflected light is reflected and scattered from the fog cloud toward the observer, resulting in the nearly horizontal polarization ($+45^\circ < \alpha < +135^\circ$) of light from the water-sky (Figs. 3C and 4C).

On the basis of the above analysis it follows that if there is a celestial bright band below the water-sky, there is a maximum difference in the direction of polarization between the ice-sky and the water-sky if the latter occurs in front of nearly vertically polarized ice-sky regions. This difference becomes smaller as the angle of polarization of ice-sky light deviates from the vertical, and the difference diminishes if the background of the water-sky is a nearly horizontally polarized celestial area.

A not-directly-visible polynya can be detected from a distance by means of the water-sky visible above it. The water-sky itself can be recognized on the basis of either the smaller radiance or the larger or smaller difference in the angle of polarization relative to the ice-sky. Arctic birds (if sensitive to polarization) could detect water-skies by means of polarization only if the threshold of their polarization sensitivity were as low as $\sim 10\%$, because the degree of linear polarization of water-skies is not higher than 10% (Tables 2 and 3). We admit, however, that it is

unknown yet whether any arctic bird species is polarization sensitive.

ACKNOWLEDGMENTS

The financial support received by S. Åkesson and G. Horváth from the Swedish Polar Research Secretariat (SPRS) and from the Swedish Research Council to S. Åkesson is very much appreciated. Many thanks to Anders Karlqvist (director of the SPRS, Stockholm), who made it possible for S. Å. and G. H. to attend the Beringia 2005 expedition. We are grateful to Sven Stenvall (helicopter pilot, SPRS, Kallaxflyg) for his logistical help. Thanks to Rüdiger Wehner (Department of Zoology, University of Zürich, Switzerland) for lending his Nikon fisheye lens used in our imaging polarimeter. Thanks to Balázs Bernáth for the statistical analyses.

Author contact information is as follows: Ramón Hegedüs and Gábor Horváth: Biooptics Laboratory, Department of Biological Physics, Physical Institute, Loránd Eötvös University, H-1117 Budapest, Pázmány Péter sétány 1, Hungary. Susanne Åkesson: Department of Animal Ecology, Lund University, Ecology Building, SE-223 62 Lund, Sweden. Corresponding author: Gábor Horváth, e-mail address: gh@arago.elte.hu.

REFERENCES

1. I. Stirling, "The biological importance of polynyas in the Canadian Arctic," *Arctic* **33**, 303–315 (1980).
2. I. Stirling and H. Cleator (eds.), "Polynyas in the Canadian Arctic," *Occas. Pap. Can. Wildl. Serv.* **45**, 1–70 (1981).
3. I. Stirling, "The importance of polynyas, ice edges, and leads to marine mammals and birds," *J. Mar. Syst.* **10**, 9–21 (1997).
4. A. Ancel, G. L. Kooyman, P. J. Ponganis, J. P. Gendner, J. Lignon, X. Mestre, N. Huin, P. H. Thorson, P. Robisson, and Y. Le Maho, "Foraging behaviour of emperor penguins as a resource detector in winter and summer," *Nature* **360**, 336–339 (1992).
5. M. Tilzer, *125 Jahre Deutsche Polarforschung* (2nd edition, Alfred-Wegener-Institut für Polar- und Meeresforschung, Bremerhaven, Germany, 1994).
6. C. P. McRoy and J. J. Goering, "Annual budget of primary production in the Bearing Sea," *Mar. Sci. Comm.* **2**, 255–267 (1976).
7. R. G. B. Brown and D. N. Nettleship, "The biological significance of polynyas to arctic colonial seabirds," in I. Stirling and H. Cleator (eds.), *Polynyas in the Canadian Arctic. Can. Wildl. Serv. Occas. Pap.* **45**, 59–65 (1981).
8. H. J. Hirche, M. E. M. Baumann, G. Kattner, and R. Gradinger, "Plankton distribution and the impact of copepod grazing on primary production in Fram Strait, Greenland Sea," *J. Mar. Syst.* **2**, 477–494 (1991).
9. I. Stirling, D. Andriashek, and W. Calvert, "Habitat preferences of polar bears in the Western Canadian Arctic in late winter and spring," *Pol. Res.* **29**, 13–24 (1993).
10. K. Born, Ø. Wiig, and J. Thomassen, "Seasonal and annual movements of radio-collared polar bears (*Ursus maritimus*) in northeast Greenland," *J. Mar. Syst.* **10**, 67–77 (1997).
11. G. Horváth, and D. Varjú, *Polarized Light in Animal Vision—Polarization Patterns in Nature* (Springer-Verlag, 2003).
12. J. Gál, G. Horváth, V. B. Meyer-Rochow, and R. Wehner, "Polarization patterns of the summer sky and its neutral points measured by full-sky imaging polarimetry in Finnish Lapland north of the Arctic Circle," *Proc. R. Soc. London, Ser. A* **457**, 1385–1399 (2001).